Nucleosome contact triggers conformational changes of Rpd3S driving high affinity H3K36me nucleosome engagement

Chun Ruan[1], Chul-Hwan Lee[1], Haochen Cui[1], Sheng Li[2] and Bing Li[1*]

Correspondence to: Bing4.Li@utsouthwestern.edu

Supplemental Information:

Supplemental Experimental Procedures

Construction of plasmids and yeast strains:

All plasmids and yeast strains were constructed using standard procedures, and they are listed in Supplemental Tables S1 and S2.

To systematically test the cryptic transcription phenotype caused by mutations in Rpd3S, we constructed a yeast reporter strain using a strategy based on a previous report (Cheung et al., 2008). In our case, the *STE11* locus was chosen because regulation of its cryptic promoter is very sensitive to mutations in the Set2-Rpd3S pathway. First, in a Δ*RCO1* background (YBL534), the 3'ORF region of *STE11* (starting from +1870, relative to *STE11* +1 ATG) was replaced with an I-CORE cassette that includes KanMX4 and URA3 selection markers according to the *delitto perfetto* approach (Storici and Resnick, 2006), which generated the yeast strain YCR232. The knock-in cassettes that contain the *HIS3* reporter flanked by different homologous sequences of the *STE11* gene were PCR amplified from pRS313 and transformed into YCR232 to integrate the HIS3 reporter at desired *STE11* locations. The integration sites were selected such that the *HIS3* gene is out of frame with relation to the *STE11* coding region, and the functional His3 can only be produced when the *HIS3* transcript initiates at the cryptic promoter of *STE11*. Out of four positions that we chose based on our previous transcription start site mapping (Li et al., 2007b), the position +1870 (strain YCR239) is the only one that gave rise to a suitable strain for selection on drop-out plates.

For the *STE11* reporter stains, cells were grown in SC-Leu media until saturation. Equal numbers of cells were collected and diluted before spotting on the SC-Leu (control) and SC-His-Leu plates. As for the FACT mutants (all *spt16-11* derivatives), starting culture were grown at permissive temperature (26°C) until saturation. Diluted cells were then spotted on two SC-Leu plates with one being incubated at 26°C (control) and the other being placed at semi-permissive temperature (35°C).

Protein purification:

Recombinant Rpd3S or subcomplexes were purified from a Sf21 insect cell-based baculovirus expression system as described previously (Govind et al., 2010). Typically, 100 ml of freshly passed Sf21 cells were infected or co-infected with individual virus that encodes each subunit of Rpd3S for 48 hrs. Cells were collected and lysed in 10 ml of BV lysis buffer (50 mM HEPES pH7.9; 300 mM NaCl; 2 mM $MgCl_2$; 0.2% Triton X-100; 10% glycerol; 0.5 mM EDTA and freshly added protease inhibitors) on ice for 30 min. Cell lysates were clarified by ultra-centrifugation. Supernatants were then mixed with 200 µl anti-FLAG M2 resin (Sigma) and incubated at 4°C for 2 hr. Subsequently, beads were collected and washed three times with 10 ml of BV lysis buffer and eluted with 600 µl of 500 µg/ml 3xFlag peptides in BV elution buffer (50 mM HEPES pH7.9; 100 mM NaCl; 2 mM $MgCl_2$; 0.02% NP40 and 10% glycerol). If tandem purification was needed, 5 volumes of BV Lysis buffer were added back to the FLAG eluents and then mixed with 200 µl of anti-HA-agarose (Sigma) at 4°C for 2 hr. After three washes with BV lysis buffer, the proteins were eluted using 600 µl of 500 µg/ml 2xHA peptides in BV elution buffer. All final purified proteins were concentrated using Amicon concentrators. For the reconstituted recombinant Rpd3S complex, single-step purification (either through Flag-Sin3 or Flag-Rco1) should yield >90% purity of the complex that contains stoichiometric amounts of each subunit (Govind et al., 2010).

Bacterially expressed proteins (GST-Eaf3, Eaf3 truncations and various forms of Rco1-Eaf3 heterodimers) were purified essentially according to the instructions from the manufacturers. For the polycistronic expression system, most Rco1-Eaf3 heterodimers were obtained by Ni-NTA resin (QIAGEN) and glutathione beads (GE Health) tandem purification, except the proteins used in Fig. 1G-J in which only Ni-NTA affinity columns were used. To produce the AID mutants and corresponding WT of Rco1-Eaf3 heterodimers (Fig. 4G), the Ni-

NTA eluents were dialyzed into storage buffer (25 mM Tris-HCl pH8.0; 50 mM NaCl; 10 mM βME; 10% glycerol), then bound to glutathione beads. After extensive washing, TEV proteases (Invitrogen) were used to cleave the PHD-SID/Eaf3 heterodimers from beads and remove the GST-tag from Eaf3 proteins. The heterodimers were further purified through FLAG resin via a c-terminal FLAG tag of Eaf3 in order to remove TEV proteases. All final purified recombinant proteins were dialyzed or buffer-exchanged into the storage buffer and concentrated.

The concentrations of all proteins/protein complexes were determined by quantifying the band intensity of each protein on a Coomassie staining gel and comparing to common protein standards. When direct comparisons were made, each component involved was quantified on the same gel side-by-side to minimize the errors.

Chromatin immunoprecipitation (ChIP):

200 ml of each yeast culture (OD~0.8) were cross-linked using 1% formaldehyde for 15 minutes at room temperature. ChIP experiments were performed essentially as described in (Li et al., 2007a; Li et al., 2007b) using an antibody against pan-acetylated histone H4 (AcH4) (Upstate, 06-866). The primers for amplicons at coding regions of two model genes are P1403 (GATTGGGGTTGCGTATTTGCATAAG), P1404(GATGCTGCAGCAATTCAAGGGC) for *STE11*, and P1503 (CCTCATCATGGTTGGTCGCTTTGTG) , P1504 (GCATCAACCATCGTGGCTATGGTAC) for *PCA1*. A gene desert (the Y region) on Chromosome 6 where no K36me3 was detected in wild type cells and no AcH4 change was observed in Δ*SET2* (Li et al., 2007b) was chosen to serve as an internal control for quantitative PCR. Primers for amplifying the Y region are P2047 (AGTTCGAGGTAAGACCAGGTGCAAGGA) and P2048 (CGGAATATCTTCCATGCCAGTTGTTTCA). IP efficiency equals to the intensity of each IP signals divided by that of input DNA. The relative enrichment of AcH4 at *STE11* and *PCA1* were determined by normalizing their IP efficiency to that of the Y region. Error bars represent standard deviation from at least three independent experiments.

Supplemental Figures:

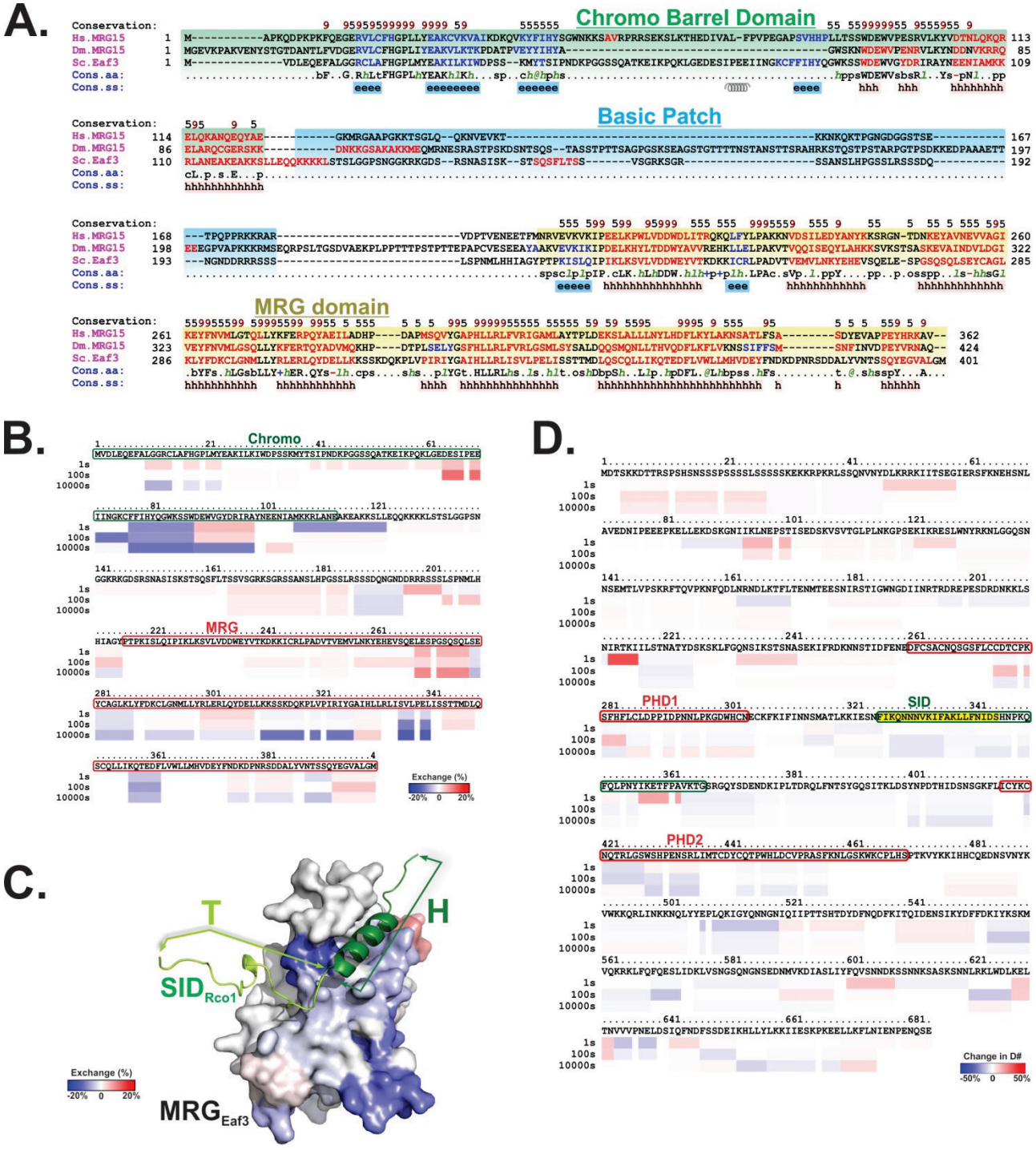

Figure S1. Deuterium exchange results of Rpd3S in free and nucleosome-bound forms, Related to Figure 1.

(A) Sequence alignment of Eaf3 and its homologues. Sequence alignment of yeast Eaf3, fly MRG15 and human MRG15 were performed using PROMALS3D (PROfile Multiple Alignment with predicted Local Structure and 3D constraints) web service. The border of the chromobarrel domain (green shade) here was extended to include the entire α-helix as predicted by the program. The Basic Patch (blue shade) coincides with the mapped DNA-Binding Region (DBR) of Eaf3. **(B)** One-dimensional maps of the Eaf3 subunit after indicated incubation time. Colored bars represent the levels of deuterium incorporation at each residue, which range from 10% (blue) to 90% (red). Higher incorporation suggests faster H/D exchange and more solvent accessibility at the region. Highlighted boxes in (B-D) indicate the regions that each domains cover. **(C)** Deuterium exchange results were mapped to 3D structure of the MRG/SID as described in Figure 1C. MRG is in surface display. SID is represented in cartoon and green. The helix region of SID (dark green) is defined as the "H" region and the turn region (light green) is referred to as "T". **(D)** One-dimensional maps of deuterium incorporation changes of Rco1 upon Rpd3S binding to nucleosome.

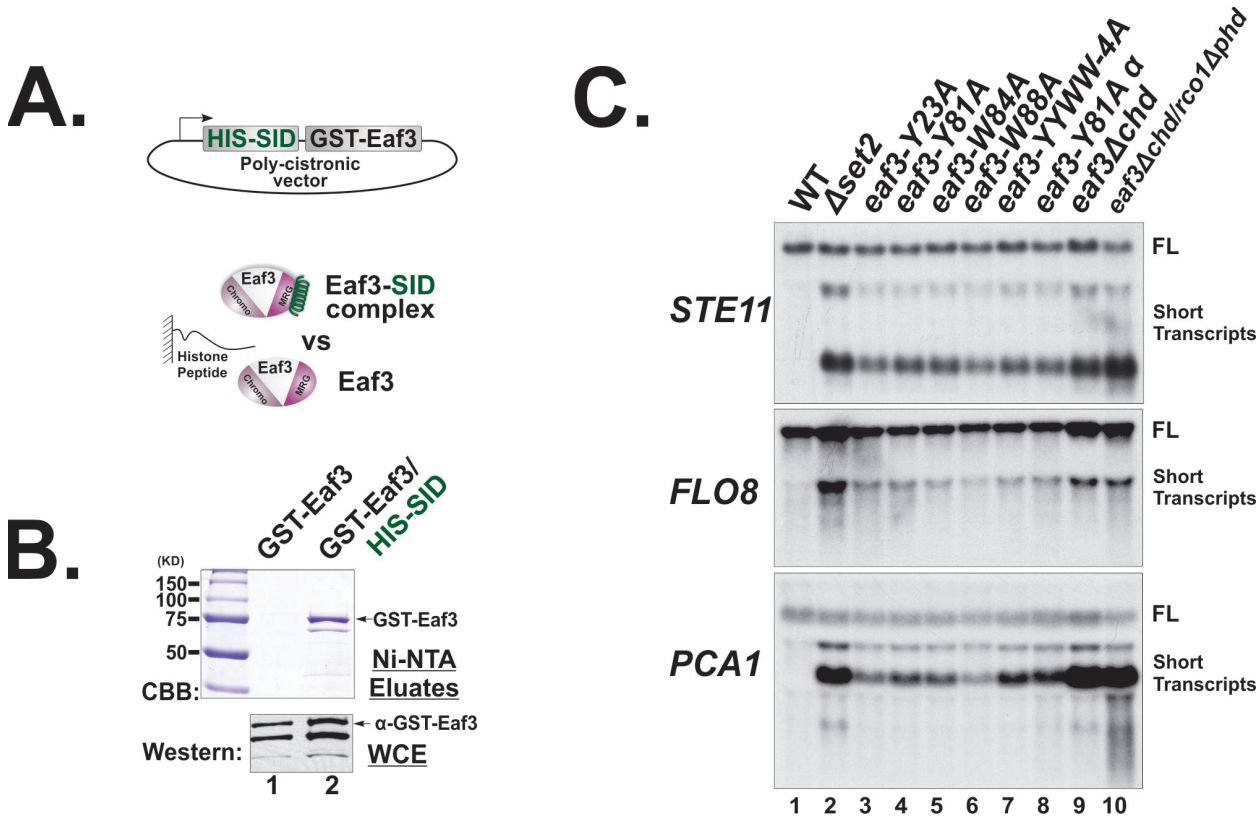

Figure S2. The critical roles of Eaf3 in Rpd3S function. Related to Figure 2.

(A) A strategy to test if SID stimulates the binding of Eaf3 to histone peptides. HIS-SID/GST-Eaf3 was co-expressed using a polycistronic vector and purified through a Ni-NTA column. GST-Eaf3 was prepared through standard GST-purification. Biotinylated histone peptides were used in histone pull-down assays. **(B)** Purification of SID-Eaf3 heterodimer. The upper panel shows the Coomassie staining of the SID/Eaf3 heterodimer (lane2); Lane 1 shows that without co-expressed HIS-SID, GST-Eaf3 does not bind to Ni-NTA column; the lower panel was the result of western blot analysis using GST antibody to demonstrate that equal amount of GST-Eaf3 was loaded on the Ni-NTA. **(C)** All four aromatic residues of CHD that form the K36me-binding pocket are essential for Rpd3S function in vivo. Total RNA was extracted from the indicated Eaf3 mutants, and Northern blot analyses were performed at three model genes that are known to show cryptic transcription when the Set2-Rpd3S pathway is defective.

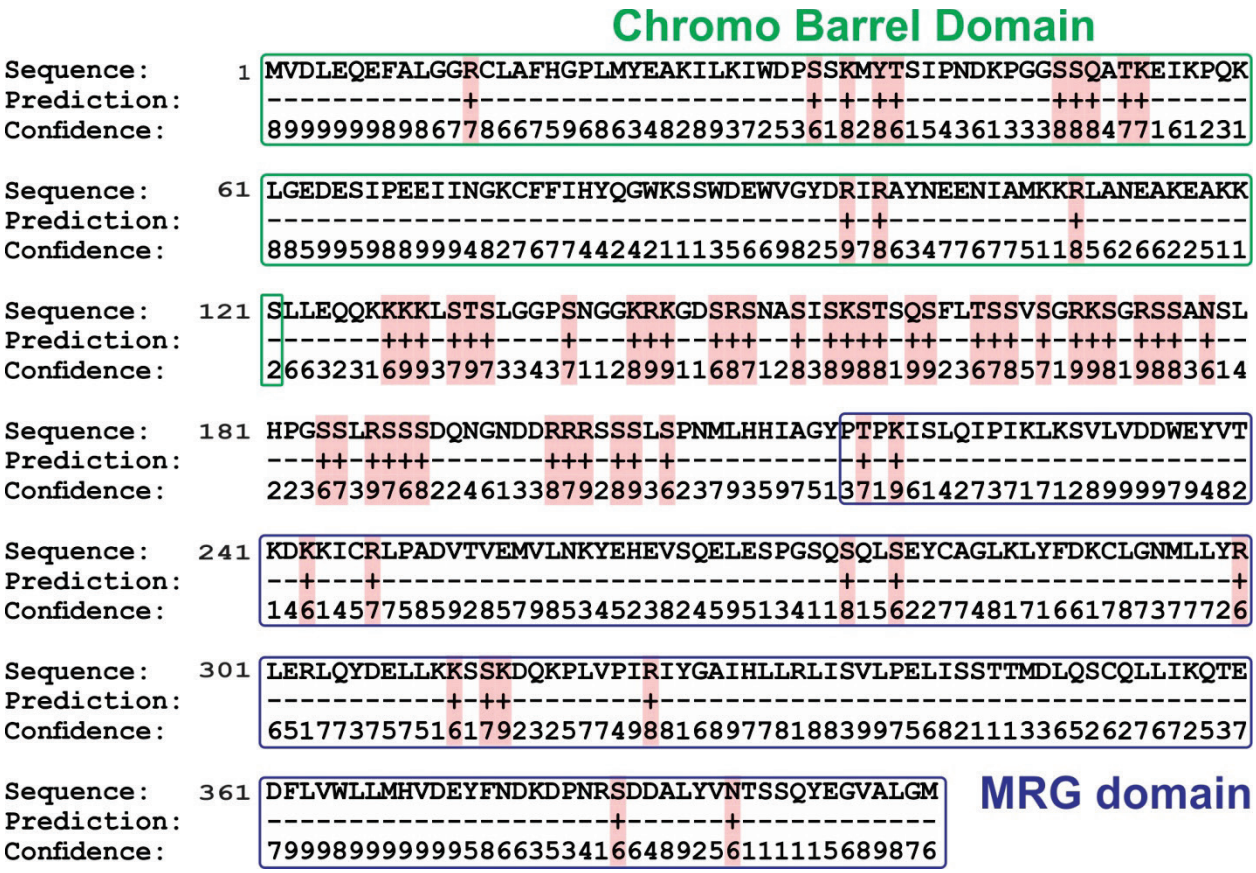

Figure S3. Predicted DNA binding residues of Eaf3. Related to Figure 3.

The residues of Eaf3 that may contribute to its DNA binding ability is predicted using BindN (http://bioinfo.ggc.org/bindn/) web server. Predicted DNA binding residues are labeled with '+'and highlighted in red, and non-binding residues are labeled with '-'. The confidence parameters were indicated ranging from 0 (lowest) to 9 (highest). Highlighted boxes indicate the regions that each domains cover.

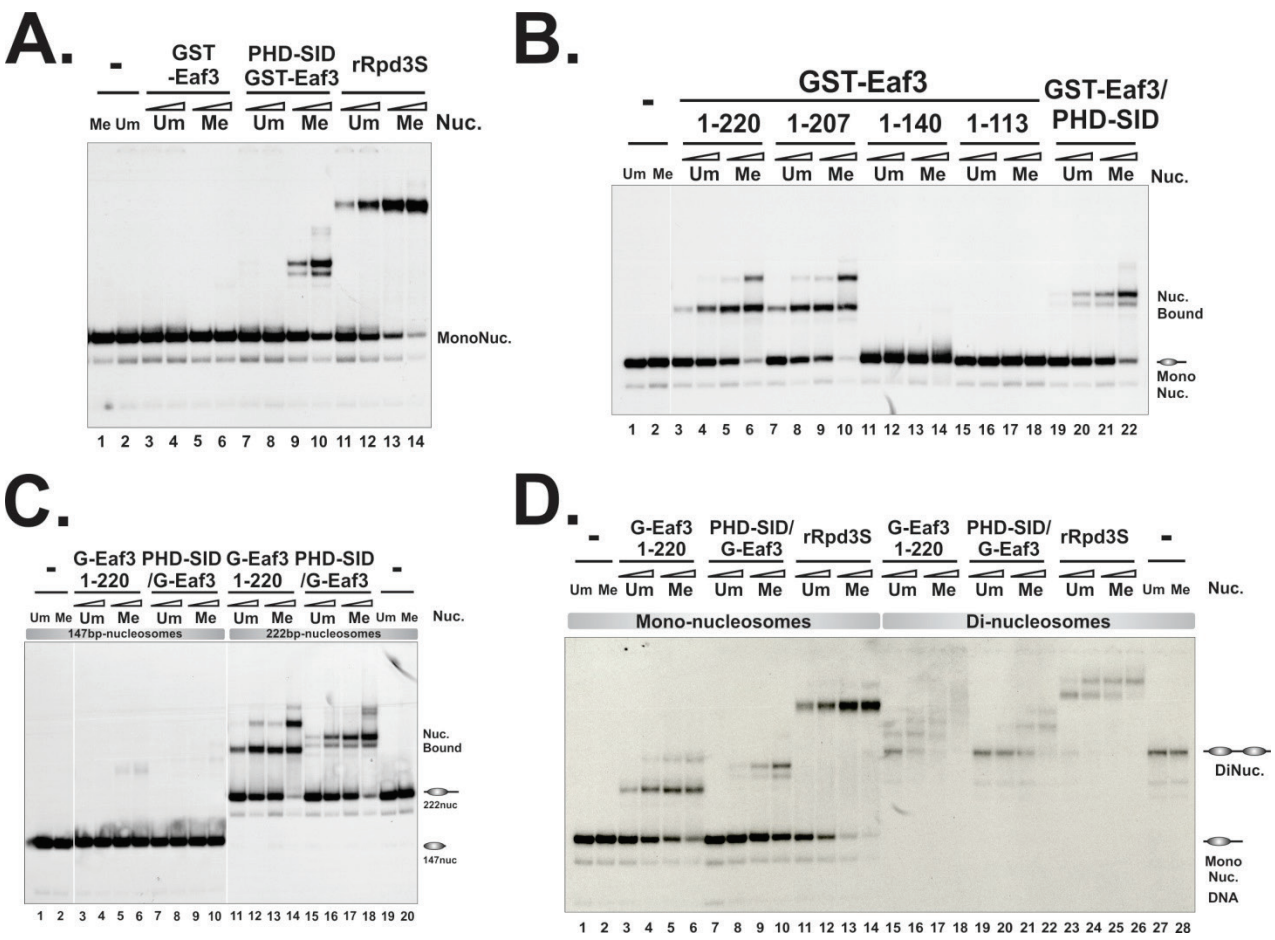

Figure S4. The binding of the Rpd3S submodules to nucleosomes as measured in EMSA. Related to Figure 3.

(A) Eaf3 protein does not bind to nucleosomes and DNA (as indicated by minimal changes of dissociated free DNA probes in lane 3-6). Full-length GST-Eaf3 was prepared from a bacteria system. When bacterially expressed GST-Eaf3 was purified through a single-step glutathione-affinity method, it resulted in co-purification of degraded Eaf3 forms (cleaved at around 220 amino acids), which can interfere with several assays reported here. A DEAE-Sepharose column and salt-gradient elution was used to remove this degraded form. **(B)** Truncated GST-Eaf3 proteins that contain the CHD and the DBR bind to nucleosomes in a H3K36 methylation dependent manner shown by EMSA using mono-nucleosomes. **(C)** The linker DNA is required for GST-Eaf3 (1-220) binding to mono-nucleosomes. Mono-nucleosomes without linker DNA were reconstituted using 147bp DNA containing only the 601 positioning sequence. **(D)** Di-nucleosomes provide a better interacting platform for all three forms of CHD-driven chromatin binding modules that were tested.

We noted that the binding of GST-Eaf3 (1-207) to nucleosomes is even stronger than PHD-SID/Eaf3 (Figure S4B). This is likely due to artificial dimerization mediated by GST-fusion. This

dimerized form can then utilize multi-valent interactions in synergy to bind to nucleosomes. To support this, we showed that removal of GST-tag drastically reduces the nucleosome binding (Figure 3E). Interestingly, GST-Eaf3 (1-207) binds to DNA (Figure 3D) but not to histone peptides (Figure 3D), however it binds to nucleosomes in a K36me dependent manner (Figure S4B), suggesting a major contribution from K36me-interacting CHD. We speculate that this form may represent ancient chromatin recognition unit in which CHD can be activated by DNA contact. However, adding DNA, in trans, cannot stimulate GST-Eaf3 (1-207) binding to H3K36 methylated histone peptides.

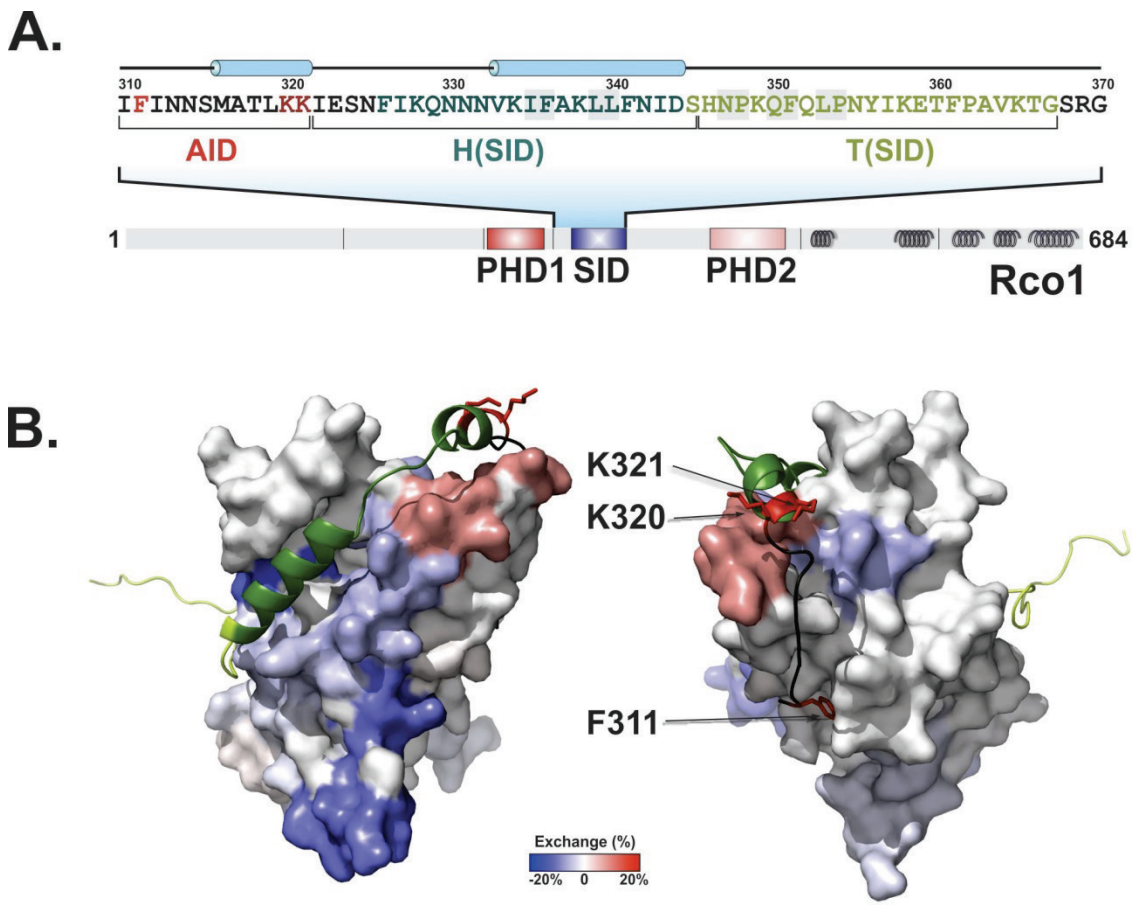

Figure S5. Molecular modeling of the AID domain of Rco1. Related to Figure 4.

(A) Domain structure of Rco1. The secondary structure prediction was performed on the PSIPRED Protein Sequence Analysis web server, which predicts an α-helix within AID, labeled as a cylinder structure on top of the protein sequence. **(B)** Structural modeling of $AID_{Rco1}$was conducted using the Coot program. The resulting model was displayed on the difference map of MRG_{Eaf3} from DXMS analysis as shown in Figure 1E using PyMOL. This model has taken into account the following factors: i) F311 can snuggly fit into a deep pocket; ii) Two lysines (labeled in red) can interact with several acidic residues within the red areas (which become more solvent-exposed upon Rpd3S binding to nucleosomes) and the blue areas (which become more protected) on MRG. These two configurations might reflect two physiological states of AID. Only one state is shown in the current model.

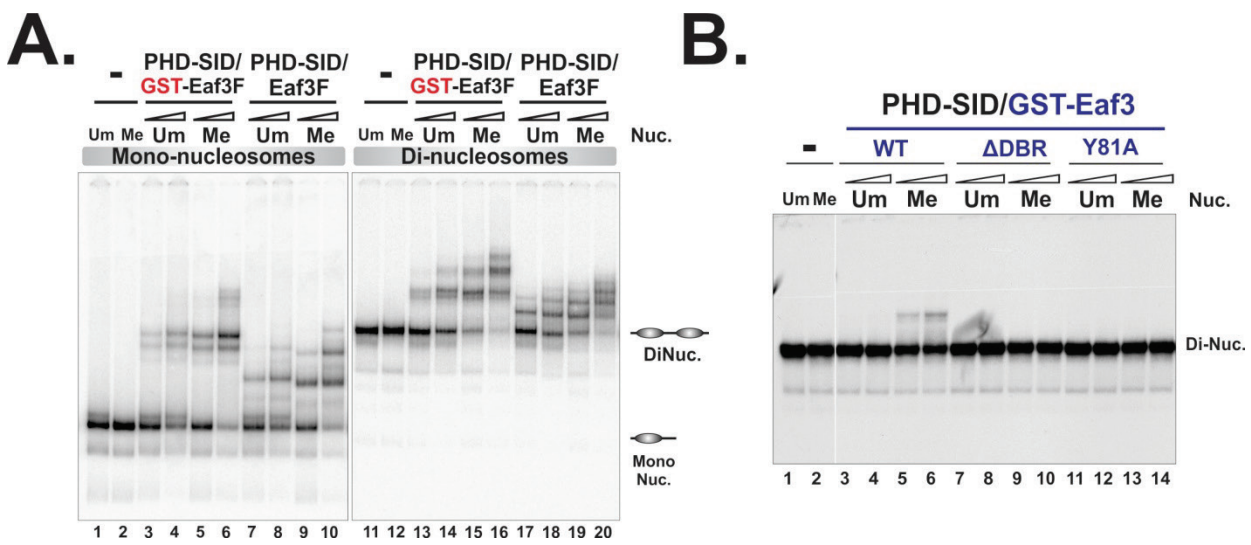

Figure S6. The binding of Rpd3S minimal recognition modules to nucleosomal substrates is not influenced by fusing to GST. Related to Figure 5.

(A) PHD-SID/GST-Eaf3F heterodimers were expressed using pBL1234, and purified through Ni-NTA and GST tandem purification as described in the supplementary experimental procedures. GST-tag was then removed by TEV cleavage; the resulting heterodimers were further purified through anti-FLAG resin to remove TEV protease. Mono-nucleosomes (196-1X) and Di-nucleosomes (196-2X) were used in EMSA assay. The result suggest that, unlike GST-Eaf3(1-220) whose nucleosome binding was dramatically enhanced through GST-mediated dimerization, GST-fusion version of the heterodimer did not increase its nucleosome binding. The binding of both versions of heterodimers was stimulated by H3K36 methylation. **(B)** The DBR and the aromatic pocket of CHD are required for the binding of PHD-SID/Eaf3 heterodimer to di-nucleosomes.

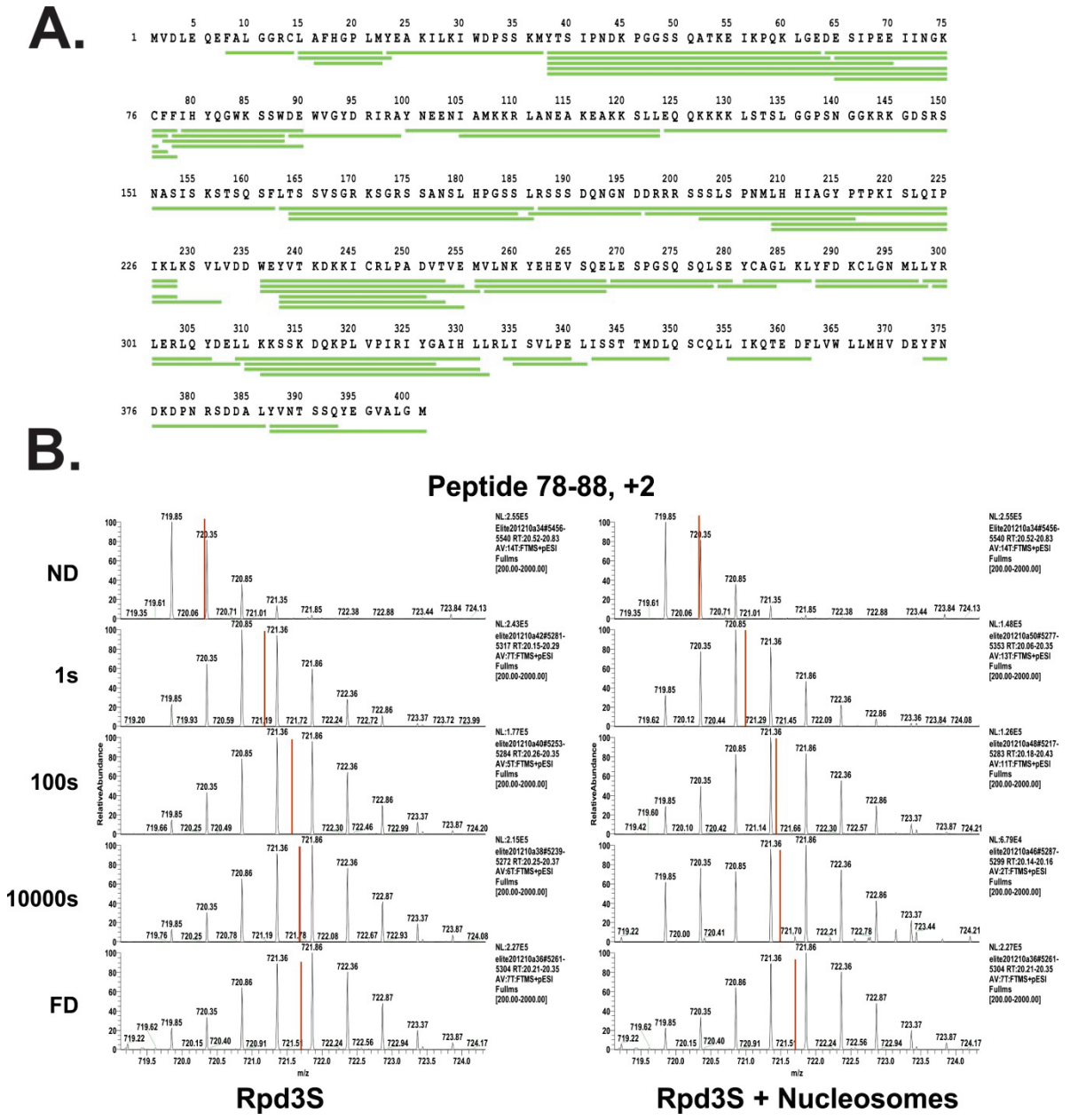

Figure S7. DXMS analysis of Rpd3S and Rpd3S-nucleosome complex. Related to Figure 1.
(A) A coverage map of Eaf3 peptides that were detected in DXMS experiments. Solid green lines indicated the fragmentation pattern of Eaf3 after pepsin digestion. **(B)** Mass Spectra of representative peptides (residue 77-88) within the CHD region in the presence (right) or absence (left) of nucleosomal substrates. Each red line represents the centroid value of corresponding isotopic envelope (Burns-Hamuro et al., 2005). ND represents non-deuterated samples, while FD depicts equilibrium-deuterated (or fully deuterated) samples. 1s, 100s and 10000s indicates the seconds that samples were exposed to deuteration prior to quenching. The reduction of peak centroid (shifting left) was observed at all three time points upon Rpd3S contact with nucleosomes.

Supplemental Table S1. Plasmid construction. Related to Figure 1-7.

Plasmids	Backbone	Description	Source
pBL471	pCR-Blunt	***pCR-RCO1-Yng2PHD (224-280)***	*(Li 2007 Science)*
pBL489	pST39	***pST39-adaptor1DCM/adaptor2***	J. Workman
pBL499	pBL503	*pST39-A1(GST-Eaf3)/A2(Φ)*	this study
pBL503	pBL489	***pST39-A1:version2/adaptor2 (A1/A2)***	this study
pBL532	pBacPak8	*pBacPak8-N-HisFlag-TEVsite*	J. Conaway
pBL541		*pBacPak8*	J. Conaway
pBL544	pBacPak8	*pBacPak8-N-2HA*	J. Conaway
pBL551	pBL532	*pBacPak8-N-HFT-Sin3*	this study
pBL552	pBL532	*pBacPak8-N-HFT-Rco1*	this study
pBL556	pBL541	*pBacPak8-Sin3*	this study
pBL557	pBL541	*pBacPak8-Rco1*	this study
pBL558	pBL541	*pBacPak8-Ume1*	this study
pBL559	pBL541	*pBacPak8-Rpd3*	this study
pBL560	pBL541	*pBacPak8-Eaf3*	this study
pBL562	pBL544	*pBacPak8-2HA-Rco1*	this study
pBL565	pBL544	*pBacPak8-2HA-Eaf3*	this study
pBL1058	pBL532	*pBacPak8-HFT-ΔSID*	this study
pBL1105	pBL503	*pST39-A1(6HIS-SID)/A2(Φ)*	this study
pBL1114	pRS415	*pRS-RCO1 expression-N-Flag Xho/Not (Rco1pro-Flag)*	this study
pBL1165	pBL1104	*pST39-A1(6HIS-**SID:Rco1 322-370**)/A2(GST-Eaf3)*	this study
pBL1169	pCR708	*pST39-A1(6HIS-**AID-SID:Rco1 310-370**)/A2(GST-Eaf3)*	this study
pBL1170	pCR708	*pST39-A1(6HiS-**PHD-SID:Rco1 260-370**)/A2(GST-Eaf3)*	this study
pBL1211	pBL1165	*pST39-A1(6HIS-PHD-ΔAID-SID)/A2(GST-Eaf3)*	this study
pBL1215	pBL869	*pRET-GST-Eaf3(1-113)*	this study
pBL1216	pBL869	*pRET-GST-Eaf3(1-140)*	this study
pBL1217	pBL869	*pRET-GST-Eaf3(1-207)*	this study
pBL1233	pBL1234	*pST39-A1(6HIS-SID)/A2(GST-Eaf3-Flag)*	this study
pBL1234	pBL1170	*pST39-A1(6HIS-PHD-SID)/A2(GST-Eaf3-Flag)*	this study
pBL1235	pBL1234	*pST39-A1(6HIS-PHD-SID:F311A)/A2(GST-Eaf3-Flag)*	this study
pBL1236	pBL1234	*pST39-A1(6HIS-PHD-SID:F311A/K320E/K321E)/A2(GST-Eaf3-Flag)*	this study
pBL1237	pBL1234	*pST39-A1(6HIS-PHD-SID K320E/K321E)/A2(GST-Eaf3-Flag)*	this study
pBL1243	pBL1234	*pST39-A1(6HIS-AID-SID)/A2(GST-Eaf3-Flag)*	this study
pBL1244	pBL541	*pBacPak8-Eaf3 ΔCHD*	this study
pBL1245	pBL541	*pBacPak8-Eaf3 Y81A*	this study
pBL1246	pBL544	*pBacPak8-HA-Rco1 ΔPHD*	this study
pBL1247	pBL499	*pST39-A1(GST-Eaf3)/A2(6HIS-SID)*	this study
pBL1249	pBL544	*pBacPak8-2HA-Rco1 L353A*	this study
pBL1250	pBL544	*pBacPak8-2HA-Rco1 ΔT*	this study
pBL1251	pBL544	*pBacPak8-2HA-Rco1 ΔH*	this study

pBL1252	pBL544	*pBacPak8-2HA-Rco1 F351A*	this study
pBL1253	pBL1114	*pRS415 Rco1pro Flag-Rco1WT*	this study
pBL1254	pBL1114	*pRS415 Rco1pro Flag-Rco1 ΔSID*	this study
pBL1255	pBL1114	*pRS415 Rco1pro Flag-Rco1 L353A*	this study
pBL1256	pBL1114	*pRS415 Rco1pro Flag-Rco1 ΔH*	this study
pBL1257	pBL532	*pBacPak8-HFT Rco1 Δ1-160*	this study
pBL1258	pBL532	*pBacPak8-HFT Rco1 Δ1-260*	this study
pBL1259	pBL532	*pBacPak8-HFT-Rco1 ΔAID*	this study
pBL1260	pBL544	*pBacPak8-2HA-Rco1 ΔAID*	this study
pBL1261	pBL1114	*pRS415-Rco1pro Flag-Rco1ΔAID*	this study
pBL1262	pBL544	*pBacPak8-2HA-Rco1 F311A*	this study
pBL1263	pBL532	*pBacPak8-HFT-Rco1 F311A*	this study
pBL1264	pBL1114	*pRS415-Rco1pro Flag-Rco1 F311A*	this study
pBL1265	pBL544	*pBacPak8-2HA-Rco1 K320E/K321E*	this study
pBL1266	pBL532	*pBacPak8-HFT-Rco1 K320E/K321E*	this study
pBL1267	pBL1114	*pRS415-Rco1pro Flag-Rco1K320E/K321E*	this study
pBL1268	pBL544	*pBacPak8-2HA-Rco1 F311A/K320E/K321E*	this study
pBL1269	pBL532	*pBacPak8-HFT-Rco1 F311A/K320E/K321E*	this study
pBL1270	pBL1114	*pRS415-Rco1pro Flag-Rco1 F311A/K320E/K321E*	this study
pBL1271	pBL869	*pRET-GST-Eaf3(1-220)*	this study
pBL1272	pBL1170	*pST39-A1(6HIS-PHD-SID:F311A/K320E/K321E)/A2(GST-Eaf3)*	this study
pBL1273	pBL1170	*pST39-A1(6HIS-PHD-SID:K320E/321E)/A2(GST-Eaf3)*	this study
pBL1274	pBL869	*pRET-GST-Eaf3*	this study
pBL1275	pBL869	*pRET-GST-Eaf3-Flag*	this study
pBL1276	pBL1235	*pST39-A1 (6HIS-PHD-SID:F311A)/A2 (GST-Eaf3)*	this study
pBL1290	pBL1288	*pBLST39 A1(6HIS-SID)/A2(GST-eaf3-Y23A,W81A,W84A,W88A) (eaf3-4A)*	this study
pBL1291	pBL1287	*pBLST39 A1(6HIS-PHD-SID)/A2-GST-eaf3-Y81A*	this study
pBL1296	pBL1293	*pBLST39 A1(6HIS-PHD-SID)/A2-GST-eaf3 ΔDBR (116-206)*	this study
pBL1353	pBL1233	*pST-A1(6His-PHDyng2-SID **Yng2:224-280-Rco1:308-370**)-A2(GST-Eaf3)*	this study

Supplemental Table S2. Yeast Strains. Related to Figure 1-7.

Strain	Parental	Description	Source
YBL534		*MAT**a**, his3Δ1 leu2Δ0 met15Δ0 ura3Δ0* ***RCO1Δ::KANMX6***	*J .Workman*
YBL555		*MAT**alpha** his3Δ1 leu2Δ0 lys2Δ 0 ura3Δ0* ***eaf3-chd77-113*****Δ Flag:Leu2**	*J .Workman*
YBL583		*MATa his3Δ1 leu2Δ0 met15Δ0 ura3Δ0* ***Rco1-TAP::HIS3MX6***	*Open Biosys.*
YBL693	**YBL675**	***MATa Rco1-ΔPhD-TAP:HIS/ eaf3Δchd1***	*J .Workman*
YBL741	YBL739	*MATa his3Δ1 leu2Δ0 met15Δ0 ura3Δ0* ***Eaf3-CHD-Y23A***	this study
YBL742	YBL739	*MATa his3Δ1 leu2Δ0 met15Δ0 ura3Δ0* ***Eaf3-CHD-Y81A***	this study
YBL743	YBL739	*MATa his3Δ1 leu2Δ0 met15Δ0 ura3Δ0* ***Eaf3-CHD-W84***	this study
YBL744	YBL739	*MATa his3Δ1 leu2Δ0 met15Δ0 ura3Δ0* ***Eaf3-CHD-W88***	this study
YBL745	YBL739	*MATa his3Δ1 leu2Δ0 met15Δ0 ura3Δ0* ***Eaf3-CHD-YYWW-AAAA***	this study
YBL746	YBL740	***MATalpha** his3Δ1 leu2Δ0 lys2Δ 0 ura3Δ0* ***Eaf3-CHD-Y81A***	this study
YBL766	w303a	*MAT**a** ura3-1 lys2Δ::hisG trp1-1 his3-11,15 leu2-3,112 can1-100* ***Rco1-TAP:HIS3MX6***	this study
YBL768	YBL766	*MATa ura3-1 lys2Δ::hisG trp1-1 his3-11,15 leu2-3,112 can1-100* ***Rco1-TAP:HIS3MX6 Eaf3-3XFlag:KAN***	this study
YBL770	w303alpha	*MATalpha ura3-1 lys2Δ::hisG trp1-1 his3-11,15 leu2-3,112 can1-100* ***Rco1-HA:TRP***	this study
YBL772	W303 diploid	*MATa ura3-1 lys2Δ::hisG trp1-1 his3-11,15 leu2-3,112 can1-100* ***Rco1-TAP:HIS3MX6*** *MATalpha ura3-1 lys2Δ::hisG trp1-1 his3-11,15 leu2-3,112 can1-100* ***Rco1-HA:TRP***	this study
YBL821	w303	*MATa ade2 can1 his3 leu2 lys2 met15 trp1 ura3* ***spt16-11***	*D. Stillman*
YBL823	w303	*MATa ade2 can1 his3 leu2 lys2 met15 trp1 ura3* ***spt16-11 RCO1Δ::URA3MX***	*D. Stillman*
YBL842	YBL821	*MATa ade2 can1 his3 leu2 lys2 met15 trp1 ura3* ***spt16-11 pBL1114 N-Flag vector***	this study
YBL843	YBL823	*MATa ade2 can1 his3 leu2 lys2 met15 trp1 ura3* ***spt16-11 RCO1Δ::URA3MX pBL1114 N-Flag vector***	this study
YBL844	YBL823	*MATa ade2 can1 his3 leu2 lys2 met15 trp1 ura3* ***spt16-11 RCO1Δ::URA3MX pBL1253-Rco1 WT***	this study
YBL845	YBL823	*MATa ade2 can1 his3 leu2 lys2 met15 trp1 ura3* ***spt16-11 RCO1Δ::URA3MX pBL1256-Rco1 HΔ***	this study
YBL846	YBL823	*MATa ade2 can1 his3 leu2 lys2 met15 trp1 ura3* ***spt16-11 RCO1Δ::URA3MX pBL1255-Rco1 L353A***	this study
YBL847	YBL823	*MATa ade2 can1 his3 leu2 lys2 met15 trp1 ura3* ***spt16-11 RCO1Δ::URA3MX pBL1254-Rco1 ΔSID***	this study
YCR232	**YBL534**	*MAT**a**, his3Δ1 leu2Δ0 met15Δ0 ura3Δ0* ***RCO1Δ::KANMX6 STE11-1870 I-CORE URA3/KAN***	this study
YCR239	YCR232	*MATa, his3Δ1 leu2Δ0 met15Δ0 ura3Δ0* ***RCO1Δ::KANMX6 STE11-1870::HIS3***	this study
YCR351	**BY4741**	*MATa his3Δ1 leu2Δ0 lys2Δ 0 ura3Δ0* ***RCO1:: I-CORE at 234aa***	this study
YCR352	**YCR351**	*MATa his3Δ1 leu2Δ0 lys2Δ 0 ura3Δ0* ***RCO1::ΔSID***	this study
YCR353	**YCR352**	*MATa his3Δ1 leu2Δ0 lys2Δ 0 ura3Δ0* ***RCO1::ΔSID-TAP-HIS3***	this study
YCR355	**YCR351**	*MATa his3Δ1 leu2Δ0 lys2Δ 0 ura3Δ0* ***RCO1:: ΔT***	this study
YCR357	**YCR355**	*MATa his3Δ1 leu2Δ0 lys2Δ 0 ura3Δ0* ***RCO1::ΔT-TAP-HIS3***	this study
YCR369	**YCR239**	*MATa, his3Δ1 leu2Δ0 met15Δ0 ura3Δ0* ***RCO1Δ::KANMX6 STE11-1870::HIS3 pBL1114-N-Flag vector***	this study
YCR370	**YCR239**	*MATa, his3Δ1 leu2Δ0 met15Δ0 ura3Δ0* ***RCO1Δ::KANMX6 STE11-1870::HIS3 pBL1253-Rco1 WT***	this study
YCR371	**YCR239**	*MATa, his3Δ1 leu2Δ0 met15Δ0 ura3Δ0* ***RCO1Δ::KANMX6 STE11-1870::HIS3 pBL1254-Rco1 ΔSID***	this study
YCR372	**YCR239**	*MATa, his3Δ1 leu2Δ0 met15Δ0 ura3Δ0* ***RCO1Δ::KANMX6 STE11-1870::HIS3 pBL1255-Rco1 L353A***	this study

YCR373	**YCR239**	*MATa, his3Δ1 leu2Δ0 met15Δ0 ura3Δ0* ***RCO1Δ::KANMX6 STE11-1870::HIS3 pBL1256-Rco1 ΔH***	this study
YCR393	**YCR239**	*MATa, his3Δ1 leu2Δ0 met15Δ0 ura3Δ0* ***RCO1Δ::KANMX6 STE11-1870::HIS3 pBL1261-Rco1 ΔAID***	this study
YCR394	**YCR239**	*MATa, his3Δ1 leu2Δ0 met15Δ0 ura3Δ0* ***RCO1Δ::KANMX6 STE11-1870::HIS3 pBL1264-Rco1 F311A***	this study
YCR395	**YCR239**	*MATa, his3Δ1 leu2Δ0 met15Δ0 ura3Δ0* ***RCO1Δ::KANMX6 STE11-1870::HIS3 pBL1267-Rco1 K320E/K321E***	this study
YCR396	**YCR239**	*MATa, his3Δ1 leu2Δ0 met15Δ0 ura3Δ0* ***RCO1Δ::KANMX6 STE11-1870::HIS3 pBL1270-Rco1 F311A/K320E/K321E***	this study

References:

Burns-Hamuro, L.L., Hamuro, Y., Kim, J.S., Sigala, P., Fayos, R., Stranz, D.D., Jennings, P.A., Taylor, S.S., and Woods, V.L., Jr. (2005). Distinct interaction modes of an AKAP bound to two regulatory subunit isoforms of protein kinase A revealed by amide hydrogen/deuterium exchange. Protein Sci *14*, 2982-2992.

Cheung, V., Chua, G., Batada, N.N., Landry, C.R., Michnick, S.W., Hughes, T.R., and Winston, F. (2008). Chromatin- and transcription-related factors repress transcription from within coding regions throughout the Saccharomyces cerevisiae genome. PLoS Biol *6*, e277.

Govind, C.K., Qiu, H., Ginsburg, D.S., Ruan, C., Hofmeyer, K., Hu, C., Swaminathan, V., Workman, J.L., Li, B., and Hinnebusch, A.G. (2010). Phosphorylated Pol II CTD recruits multiple HDACs, including Rpd3C(S), for methylation-dependent deacetylation of ORF nucleosomes. Mol Cell *39*, 234-246.

Li, B., Gogol, M., Carey, M., Lee, D., Seidel, C., and Workman, J.L. (2007a). Combined action of PHD and chromo domains directs the Rpd3S HDAC to transcribed chromatin. Science *316*, 1050-1054.

Li, B., Gogol, M., Carey, M., Pattenden, S.G., Seidel, C., and Workman, J.L. (2007b). Infrequently transcribed long genes depend on the Set2/Rpd3S pathway for accurate transcription. Genes Dev *21*, 1422-1430.

Storici, F., and Resnick, M.A. (2006). The delitto perfetto approach to in vivo site-directed mutagenesis and chromosome rearrangements with synthetic oligonucleotides in yeast. Methods in enzymology *409*, 329-345.